Oil Shale, 2017, Vol. 34, No. 1, pp. 55–69
https://doi.org/10.3176/oil.2017.1.04
ISSN 0208-189X

BIOMARKERS OF THE LOWER JURASSIC BLACK SHALE IN THE SHUANGHU AREA OF THE QIANGTANG BASIN, NORTHERN TIBET, AND THEIR GEOLOGICAL SIGNIFICANCE

GUOQING XIA[(a,b)], CHANGJUN JI[(c)*], LAN CHEN[(d)], HAISHENG YI[(a,b)]

[(a)] Institute of Sedimentary Geology, Chengdu University of Technology, Chengdu 610059, China
[(b)] State Key Laboratory of Oil/Gas Reservoir Geology and Exploitation, Chengdu 610059, China
[(c)] Chinese Academy of Geological Sciences, Beijing 100037, China
[(d)] College of Petroleum Engineering, Chongqing University of Science and Technology, Chongqing 401331, China

Abstract. *The organic-rich black shale in the Qiangtang Basin, northern Tibet, has long been the focus of petroleum geologists. This paper discusses the characteristics and maturity parameters of such biomarkers of the shale as n-alkanes, acyclic isoprenoids, terpenoids and steranes, using gas chromatographic (GS) and mass spectrometric (MS) techniques. n-Alkanes are characterized by a typical unimodal distribution, with dominant low carbon numbers of nC_{16}–nC_{19}, which suggests that the organic matter sources are mainly algae and planktonic organisms along with terrestrial higher plants. Furthermore, acyclic isoprenoid alkanes pristane (Pr) and phytane (Ph) are the most abundant, the Pr/Ph ratio being 0.06–0.70. The phytane dominance indicates that organic matter deposited in a reducing environment. In addition, the C_{31}22S/(22S + 22R) hopanes ratio is 0.58–0.59, that of C_{29}20S/(20S + 20R) regular steranes 0.43–0.59, and αββ/(αββ + ααα) 0.39–0.65. These maturity parameters show that organic matter is in the maturity stage, while it is slightly more mature in the Biluocuo (BLC) section of the Qiangtang Basin than in the Ganbeixiama (GB) section. As indicated by the biomarkers values, the Jurassic source rocks in the two researched sections have a certain hydrocarbon potential.*

Keywords: *Jurassic, black shale, biomarker, Qiangtang Basin, northern Tibet.*

* Corresponding author: e-mail *jichangjun2007@sina.com*

1. Introduction

The Qiangtang Basin in northern Tibet deposits the most complete and widely-spread Mesozoic marine sediment, which is characterized by certain oil seepages. Therefore, petroleum geologists have been paying much attention to the potential oil-gas exploration in this area [1, 2]. The researchers have established that there are five major source rocks in the basin: the Xiaochaka Formation (T_3x), the Quse Formation (J_1q,), the Buqu Formation (J_2b), the Xiali Formation (J_2x) and the Suowa Formation (J_3s), and two minor ones – the Quemocuo Formation (J_2q) and the Xueshan Formation (J_3x) [1, 2]. Characterized by the abundance of organic-rich black shale, the Quse Formation in the Shuanghu-Sewa area and the Biluocuo oil shale (maximum total organic carbon (TOC) content 26.12%) in particular have received more attention [3–8]. At the same time, other black oil shales with low TOC content have been investigated less, especially in terms of biomarkers. This paper studies two typical sections of the Qiangtang Basin – Biluocuo (BLC) and Ganbeixiama (GB), and examines in detail the biomarkers of both low- and high-TOC black shale for the abundance, type and maturity of organic matter, and sedimentary environment. The aim is to provide target regions for further oil-gas exploration in the Qiangtang Basin in northern Tibet.

2. Geological background

The Qiangtang Basin is located in the eastern Tethys between the Hoh Xil-Jinshajiang Suture Zone and the Bangong-Nujiang Suture Zone [1, 2, 9]. It is about 250 km wide (south-north) and 640 km long (east-west) with an area of about 18×10^4 km^2 [1, 10, 11]. The basin includes one uplift and two depressions: the Southern Qiangtang Depression, the Central Uplift and the Northern Qiangtang Depression, from south to north [2, 9, 12–14].

The two research sections, Biluocou and Ganbeixiama, are located in the Southern Qiangtang Depression where Jurassic strata have mainly developed, along with a small number of Upper Triassic and Cenozoic strata. The Jurassic stratum consists of the Quse Formation (J_1q), the Sewa Formation (J_2s), the Shaqiaomu Formation ($J_2\hat{s}q$), the Buqu Formation (J_2b), the Xiali Formation (J_2x), and the Suowa Formation (J_3s), from lower to upper. The stratum roughly spreads from east to west in zones from south to north, i.e. shallow water carbonate deposits are mainly developed in the Northern Qiangtang Depression next to the Central Uplift Belt, including the Buqu Formation, the Xiali Formation and the Suowa Formation, while the southern area lacks platform carbonate rocks. The shelf or basin facies black shales are primarily distributed in the Quse and Sewa Formations, with the boundaries running roughly along Geluguanna-Deruri-Quruiqianai-Ganbeixiama (Fig. 1).

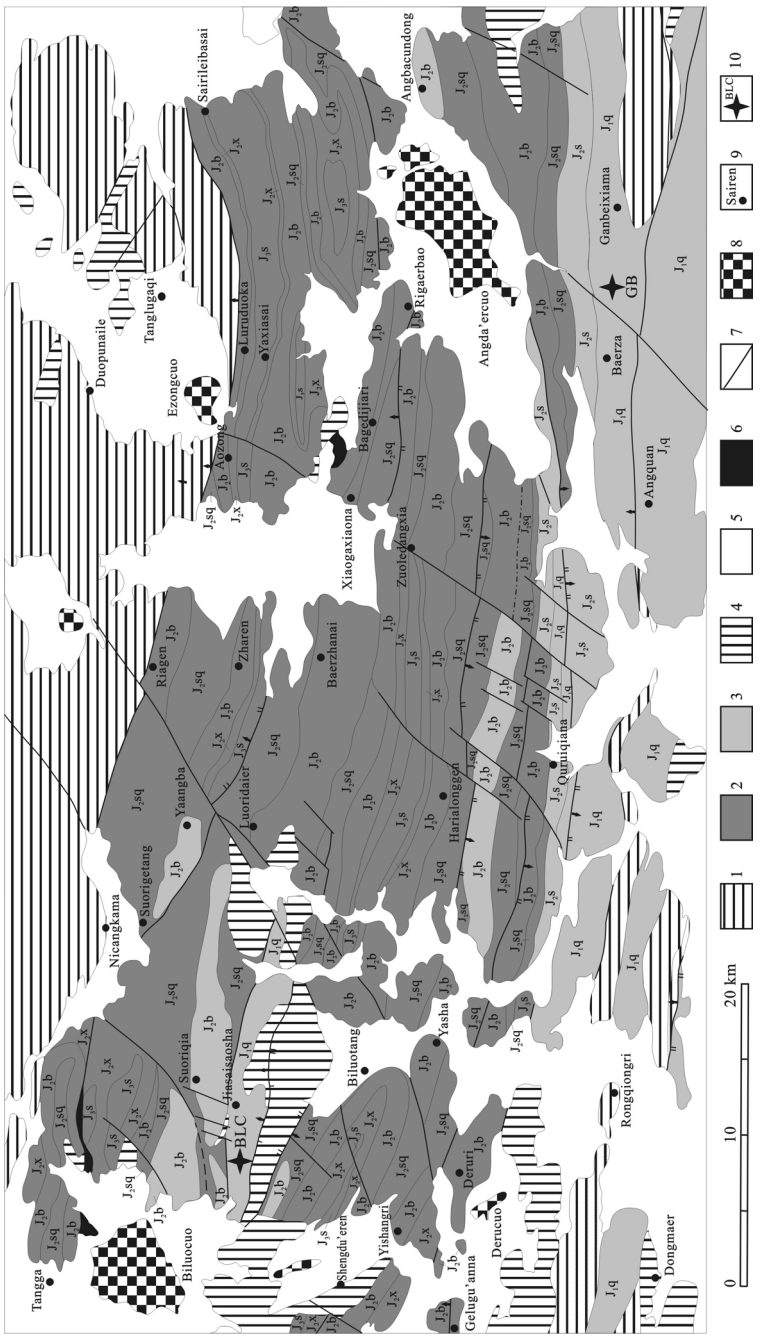

Fig. 1. Stratigraphic distribution of the Southern Qiangtang Depression and location of the research sections.

(1 – Triassic; 2 – Distribution of shallow water carbonate platforms; 3 – Distribution of mud and sand in the shelf and basin; 4 – Cretaceous; 5 – Neogene; 6 – Eocene volcanic rock; 7 – Faults; 8 – Lakes; 9 – Place names; 10 – Section and sample positions. Geological map drawn according to the 1/250,000 Angdaʼercuo regional geological map revision).

The samples for biomarker determination were collected from the Biluocuo and Ganbeixiama sections of the Qiangtang Basin (Fig. 1). The samples were labelled as indicated in Table 1. The BLC section is situated in the Jiasaisaosha area southeast of Lake Biluocuo, and the GB section is located in the south of the Angdaercuo area. In both sections, the Quse Formation is dominated by black shale interbedded with thin-layered siltstone, and argillaceous limestone containing rich ammonites and bivalves. The sediment facies is characterized by a shelf sea deposit. The ammonites include a specimen identified as an Early Toarcian *Harpoceras sp*., as such, the black shale strata can be defined as Lower Jurassic [3, 15–19].

Table 1. Geochemical data for Lower Jurassic black shale in the Qiangtang Basin

Sample No	Lithology	Chloroform asphalt A, ppm	Chloroform bitumen A component, wt%				Saturates/ aromatics	Total hydrocarbons
			Saturates	Aromatics	Non-hydrocarbons	Asphaltene		
GB05S	Shale	16.11	11.11	29.63	40.74	18.52	0.37	40.74
GB09S	Marl	16.88	24	16	40	20	1.50	40
GB10S	Shale	14.91	16.67	8.33	45.83	29.17	2.00	25
GB11S	Marl	14.03	31.82	9.09	9.09	50	3.50	40.91
BLC01S1	Oil Shale	428.57	33.79	15.52	18.62	22.76	2.18	49.31
BLC02S1	Shale	387.55	45.11	23.32	20.15	11.42	1.93	68.43
BLC02S2	Shale	653.22	32.00	20.12	18.17	29.71	1.59	52.12
BLC03S1	Mudstone	729.2	10.74	21.03	18.12	40.49	0.51	31.77
BLC03S2	Mudstone	554.62	34.55	17.11	21.30	27.04	2.02	51.66
BLC07S1	Mudstone	565.6	34.54	21.65	21.13	19.07	1.60	56.19
BLC08S1	Mudstone	507.33	35.05	20.16	21.69	23.10	1.74	55.21

3. Samples and methods

Eleven samples were taken for this study, including seven samples from the BLC section and four from the GB section (Fig. 2), the lithology was mudstone, shale, oil shale and marl. Before crushing, the samples were pretreated to remove any pollutants from their surface, washing the samples first with organic solvents and then rinsing with water to eliminate any solvent residues.

The samples were ground to 100 mesh, then reacted with dichloromethane (DCM) for 72 h in a Soxhlet apparatus to extract soluble organic fractions, before being separated. Generally, *n*-hexane was added to the soluble organic fractions, shaken up and deposited overnight for asphaltene precipitation. Next, *n*-hexane was used to rinse the saturated hydrocarbons, benzene was employed to rinse the aromatic hydrocarbons and benzene-

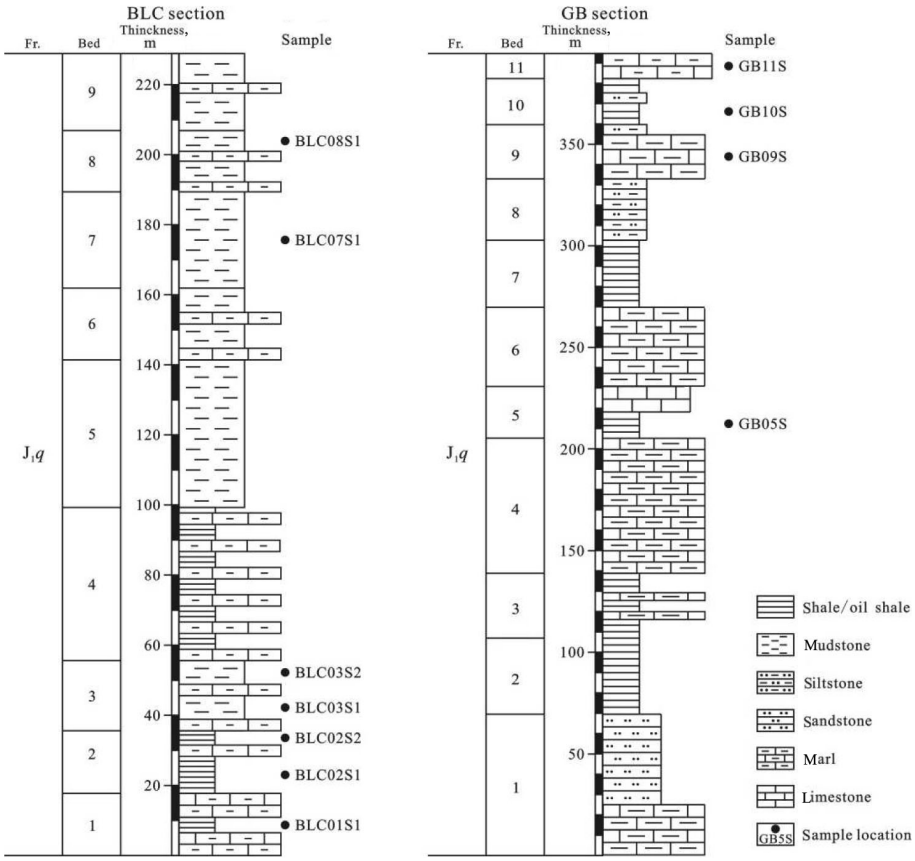

Fig. 2. Lithological columns of the research sections and sample locations. (Abbreviations used: BLC – Biluocou, GB – Ganbeixiama, Fr. – Formation).

absolute ethyl alcohol (volume ratio 1:1) was used to rinse the non-hydrocarbons. Gas chromatography-mass spectrometry (GC-MS) was performed using a Micromass Platform LC mass spectrometer equipped with an HP 6890 gas chromatograph. For the saturated hydrocarbons, a 30 m HP-5 fused silica column (0.25 mm i.d., 0.25 μm film thickness) was used with He as the carrier gas. The oven temperature was programmed from 60 °C (held for 5 min) to 290 °C (held for 20 min) at 3 °C/min. The transfer line temperature was 250 °C and the ion source temperature, 200 °C. The ion source was operated in the electron impact mode at 70 eV. All sample analyses were carried out at Yangtze University, China.

The test results are given in Table 1. As seen from the table, in the samples from the GB section, the content of chloroform bitumen A varies from 14.03 to 16.88 ppm, while this value is significantly higher in the samples from the BLC section, ranging from 387.55 to 729.2 ppm. The content of chloroform bitumen A is mostly higher than 500 ppm. Of the chloroform bitumen A components, the content of saturates in BLC samples

is relatively high, varying from 32 to 45.11% (except for sample BLC03S1 whose saturates content is 10.74%). On the contrary, the content of saturates in GB samples is relatively low, ranging from 11.11 to 24% (except for sample GB11S whose saturates content is 31.82%), and the content of aromatics is relatively high, exceeding 40% (except for sample GB11S, the aromatics content of which is 9.09%). The saturates/aromatics ratio in most samples is similar, between 1 and 3, and the total hydrocarbon content varies from 25 to 68.43 ppm.

4. Results and discussion

4.1. *n*-Alkanes and acyclic isoprenoids

A series of *n*-alkanes and acyclic isoprenoids can be detected in the total ion chromatograms (TICs) of selected samples from the GB and BLC sections of the Qiangtang Basin (Fig. 3). As is clear from the figure, the dominant carbon numbers are nC_{16}–nC_{19}, and the $\sum C_{21}-/\sum C_{22}+$ ratio changes from 0.5 to 0.99 in GB samples (except for sample GB05S whose $\sum C_{21}-/\sum C_{22}+$ is 1.39), and from 1.5 to 8.68 in BLC samples (except for sample BLC01S1, the respective ratio of which is 0.5) (Table 2). The values of odd-to-even predominance (OEP) and carbon preference index (CPI) are slightly different in the two sections. In GB, the OEP and CPI vary between 2.28 and 2.82 (except for sample GB11S with 1.05) and from 1.28 to 1.43, respectively, while in BLC, the OEP and CPI of the samples range from 0.83 to 1.13 and between 0.88 and 1.10, respectively, indicating the presence of a heavier carbon in the GB section compared with the BLC section. *n*-Alkanes with dominant carbon numbers of nC15–nC19 show the organic matter to originate from algae and planktonic organisms, while the prevailing nC_{25}–nC_{33} indicate its origin from terrigenous higher plants [20–23]. The black shales in the researched sections are characterized by the presence of low-carbon-number *n*-alkanes, which gives evidence of that the organic matter sources are algae and planktonic organisms.

The acyclic isoprenoids, especially pristane (Pr) and phytane (Ph), are abundant in all samples. The Pr/Ph ratio varies between 0.06 and 0.70 in most samples, except for samples BLC08S1 and BLC07S1 whose respective figures are 1.31 and 1.44 (Table 2). The Pr/Ph ratio was used to infer depositional redox conditions: the Pr/Ph ratio < 1 is characteristic of reducing and stratified conditions [24], while Pr/Ph > 1 is typical of oxidizing conditions [25, 26]. Furthermore, the high values of Pr/Ph (> 3.0) reflect a higher degree of oxidization and the origin of organic matter from terrigenous higher plants, while the low Pr/Ph values (< 0.6) suggest an oxygen-deficient hypersaline environment. The Pr/Ph < 0.7 of the studied samples implies a reducing environment. In addition, in BLC samples, the ratio of Ph/nC_{18} ranges from 0.32 to 0.56 and Pr/nC_{17} between 0.20 and 0.55. In GB samples, Ph/nC_{18} varies from 1.18 to 1.55 and Pr/nC_{17} between 0.64 and 0.92.

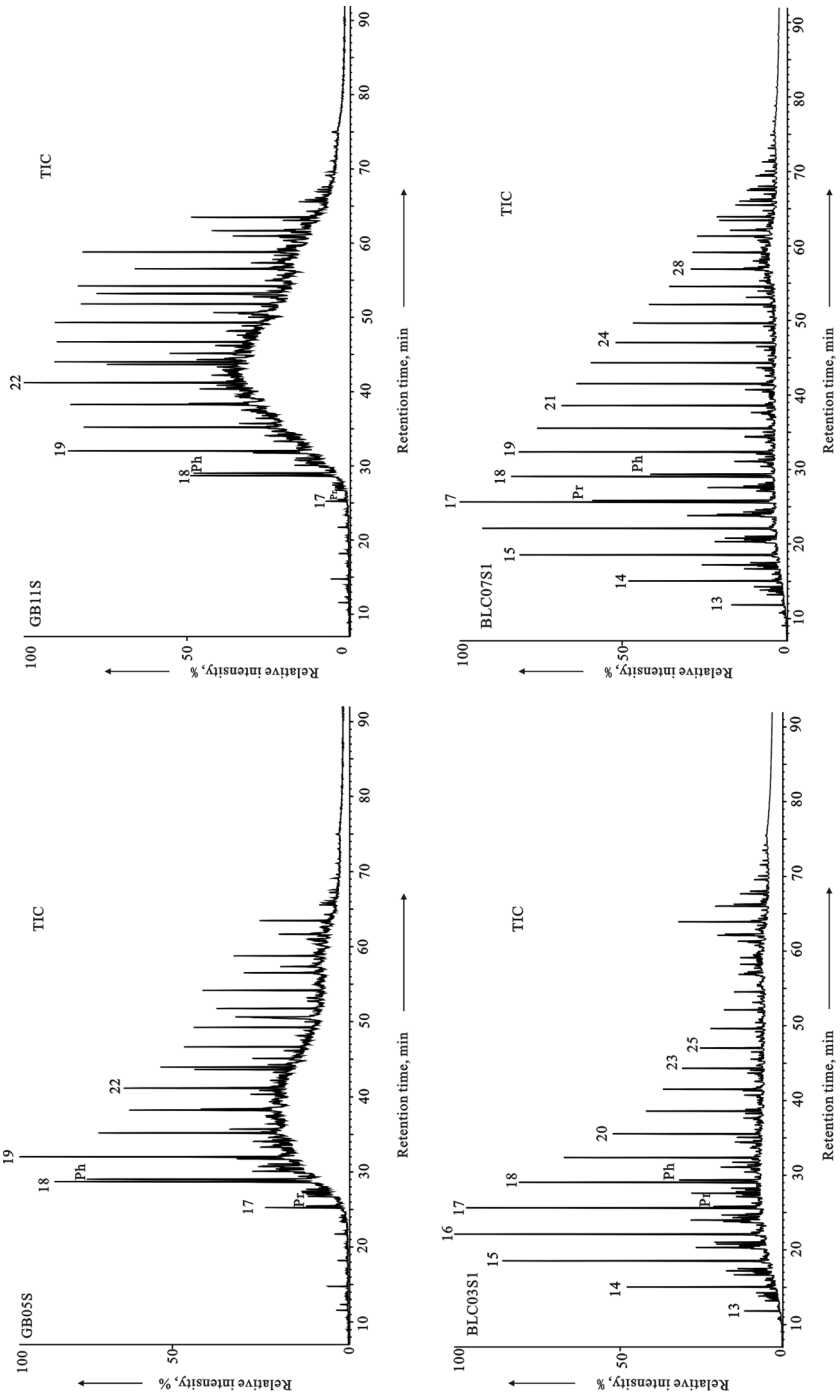

Fig. 3. Total ion chromatograms (TICs) of selected samples from the studied sections of the Qiangtang Basin. (The numbers above the chromatograms denote carbon number. Abbreviations used: GB – Ganbeixiama, BLC – Biluocou).

Table 2. Parameters of *n*-alkanes and acyclic isoprenoids of Lower Jurassic black shale in the Qiangtang Basin

Sample No	Lithology	Main peak	Carbon number	OEP	CPI	$(nC_{21} + nC_{22})/(nC_{28} + nC_{29})$	$\sum C_{21}^{-}/\sum C_{22}^{+}$	Pr/Ph	Ph/nC_{18}	Pr/nC_{17}
GB05S	Shale	nC_{19}	nC_{10}–nC_{38}	2.34	1.28	4.05	1.39	0.14	1.22	0.75
GB09S	Marl	nC_{19}	nC_{10}–nC_{38}	2.82	1.32	1.52	0.72	0.16	1.47	0.92
GB10S	Shale	nC_{19}	nC_{10}–nC_{38}	2.28	1.37	2.48	0.99	0.07	1.18	0.64
GB11S	Marl	nC_{19}	nC_{10}–nC_{38}	1.05	1.43	1.37	0.50	0.06	1.55	0.70
BL01S1	Oil Shale	nC_{18}	nC_{14}–nC_{38}	0.83	0.88	1.43	0.50	0.46	0.40	0.23
BLC02S1	Shale	nC_{16}	nC_{10}–nC_{38}	0.94	1.05	4.16	4.05	0.70	0.56	0.30
BLC02S2	Shale	nC_{17}	nC_{15}–nC_{23}	0.92	–	–	8.68	–	0.32	–
BLC03S1	Mudstone	nC_{17}	nC_{12}–nC_{38}	1.13	0.93	2.25	3.55	0.65	0.49	0.20
BLC03S2	Mudstone	nC_{16}	nC_{13}–nC_{28}	0.91	1.05	12.15	5.87	0.67	0.54	0.32
BLC07S1	Mudstone	nC_{17}	nC_{13}–nC_{37}	1.13	1.10	1.55	1.50	1.44	0.47	0.55
BLC08S1	Mudstone	nC_{16}	nC_{12}–nC_{34}	1.06	1.04	3.04	2.93	1.31	0.51	0.53

4.2. Terpenoids

The m/z 191 chromatograms of terpenoids are shown in Figure 4. The abundance of terpenoids, including pentacyclic triterpanes, tricyclic and tetracyclic terpanes, and gammacerane, can be recognized in all samples. The carbon numbers of pentacyclic triterpanes range between C_{27} and C_{35}, with C_{30} hopance as the dominant number. The $C_{31}\alpha\beta$22S/(22S + 22R) homohopane ratio is 0.58–0.59 in most samples (except for sample BLC01S1 whose respective value is 0.61), while the ratios of BLC samples are slightly higher than those of GB samples, which indicates that shale and/or oil shale are in the maturity stage (Table 3). Additionally, oleanane, lupine or other non-hopanoids, which suggest land to be the organic matter source, were not detected. At the same time, gammacerane was detected in the m/z 191 chromatograms, although in low abundance. Gammacerane may originate from protist, which is a tetrahymena and also a reliable index for indicating sedimentary environment salinity and water body stratification [27–29]. The gammacerane/$\alpha\beta C_{30}$ hopane ratio is less than 0.23 in the BLC section, being lower than that in the GB section, implying that water body salinity during sedimentation in the studied areas was normal. This finding is consistent with OEP values and phytane dominance.

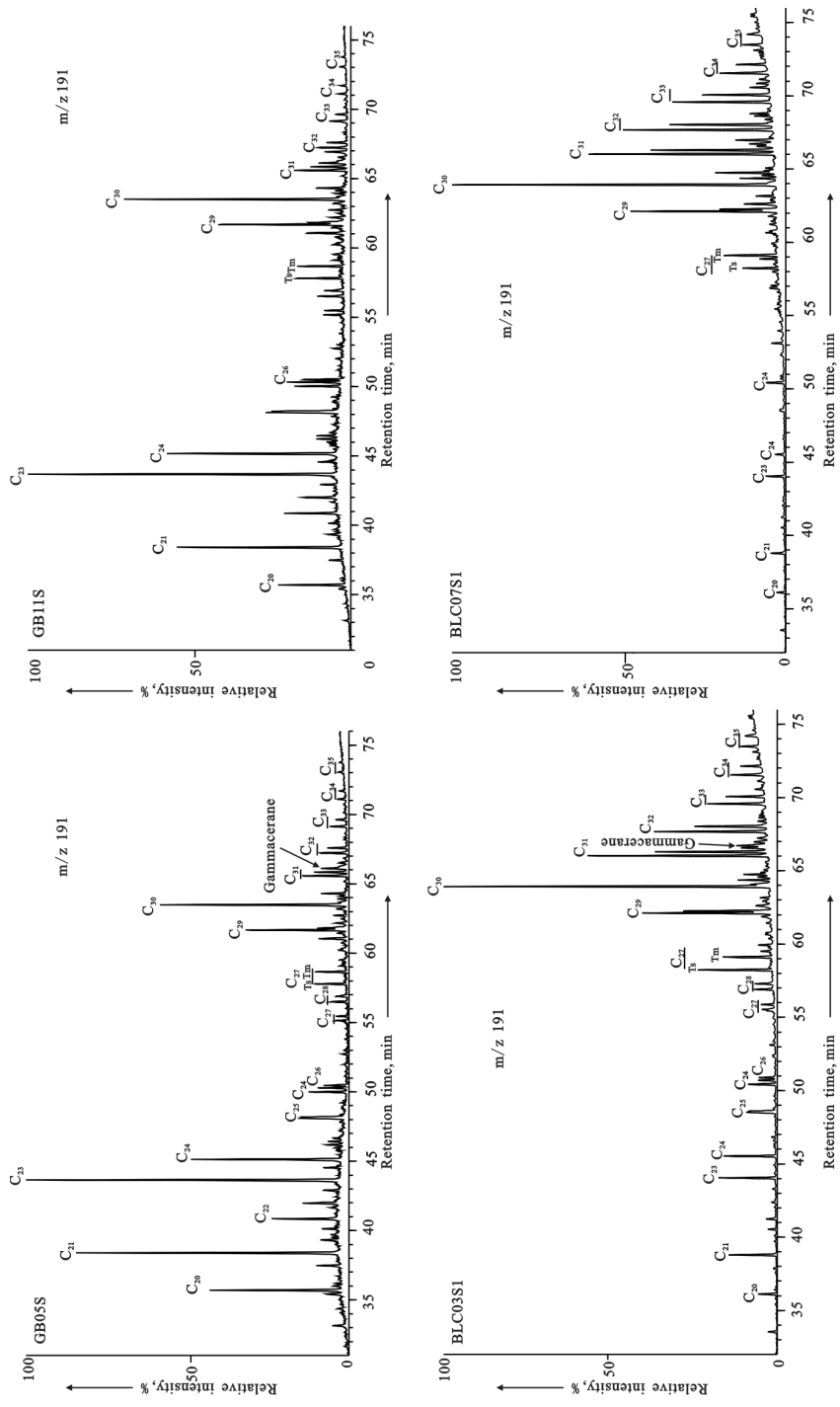

Fig. 4. m/z 191 chromatograms showing the relative abundance of terpenoids in the selected samples from the studied sections of the Qiangtang Basin. (Abbreviations used: GB – Ganbeixiama, BLC – Biluocou).

Table 3. Parameters of terpenoids of Lower Jurassic black shale in the Qiangtang Basin

Sample No	Lithology	C_{19}–C_{29} tricyclic terpanes			Tricyclic terpanes/ gammacerane	C_{29}Ts/hopane	C_{31}22S/(22S + 22R)	Gammacerane/ $C_{30}\alpha\beta$ hopane
		C_{19}–C_{22}/hopane	C_{23}–C_{26}/hopane	C_{28}–C_{29}/hopane				
GB05S	Shale	2.37	2.92	0.27	5.56	0.20	0.58	0.23
GB09S	Marl	2.02	3.33	0.34	5.69	0.20	0.58	0.17
GB10S	Shale	1.99	2.85	0.27	5.12	0.20	0.58	0.23
GB11S	Marl	1.25	2.99	0.39	4.63	0.21	0.58	0.15
BLC01S1	Oil Shale	0.33	0.65	0.29	1.27	0.22	0.61	0.11
BLC02S1	Shale	0.34	0.74	0.28	1.35	0.31	0.59	0.11
BLC02S2	Shale	0.45	0.62	0.17	1.24	0.24	0.59	0.09
BLC03S1	Mudstone	0.26	0.57	0.19	1.02	0.28	0.59	0.12
BLC03S2	Mudstone	0.20	0.39	0.16	0.74	0.26	0.59	0.12
BLC07S1	Mudstone	0.10	0.14	0.09	0.33	0.18	0.59	0.08
BLC08S1	Mudstone	0.08	0.15	0.09	0.32	0.19	0.58	0.06

Tricyclic terpanes are also found in the m/z 191 chromatograms, with carbon numbers ranging from C_{19} to C_{29} and the main peak of C_{23}. In general, tricyclic terpanes are more abundant than hopane. In GB samples, the ratio of tricyclic terpanes/gammacerane is in the range of 4.63–5.69, being 1.02–1.35 in BLC samples (except for samples BLC03S2, BL07S1 and BLC08S1 whose respective values are 0.74, 0.33 and 0.32) (Table 3), suggesting that the generative kerogen of long-chain tricyclic terpanes comes from bacteria as well as certain algae [30]. In addition, C_{24} tetracyclic and C_{26} tricyclic terpanes of bacterial source are highly abundant.

4.3. Steranes

Regular steranes (C_{27}–C_{29}), diasteranes (C_{27}–C_{29}), 4-methyl steranes (C_{28}–C_{30}) and pregnanes (C_{21}–C_{22}) are present in the m/z 217 chromatograms (Fig. 5). Furthermore, the regular steranes show a V-type distribution in all samples. In GB samples, the relative contents of C_{27}, C_{28} and C_{29} regular steranes are respectively 34–36, 28–31 and 35–35%, the $\Sigma C_{27}/\Sigma C_{29}$ ratio fluctuates from 0.99 to 1.11 (Table 4). At the same time, in BLC samples, the abundances of C_{27}, C_{28} and C_{29} regular steranes are respectively 27–41, 24–32 and 35–44%, and the $\Sigma C_{27}/\Sigma C_{29}$ ratio is in the range of 0.65–0.93 (except for sample BLC02S2 whose $\Sigma C_{27}/\Sigma C_{29}$ is 1.2, see Table 4). The source of C_{27} sterane is lower hydrobionts such as algae, while the main source of C_{29} sterane is terrigenous higher plants [31, 32]. Therefore, the organic matter source of the Lower Jurassic black shale in the Qiangtang

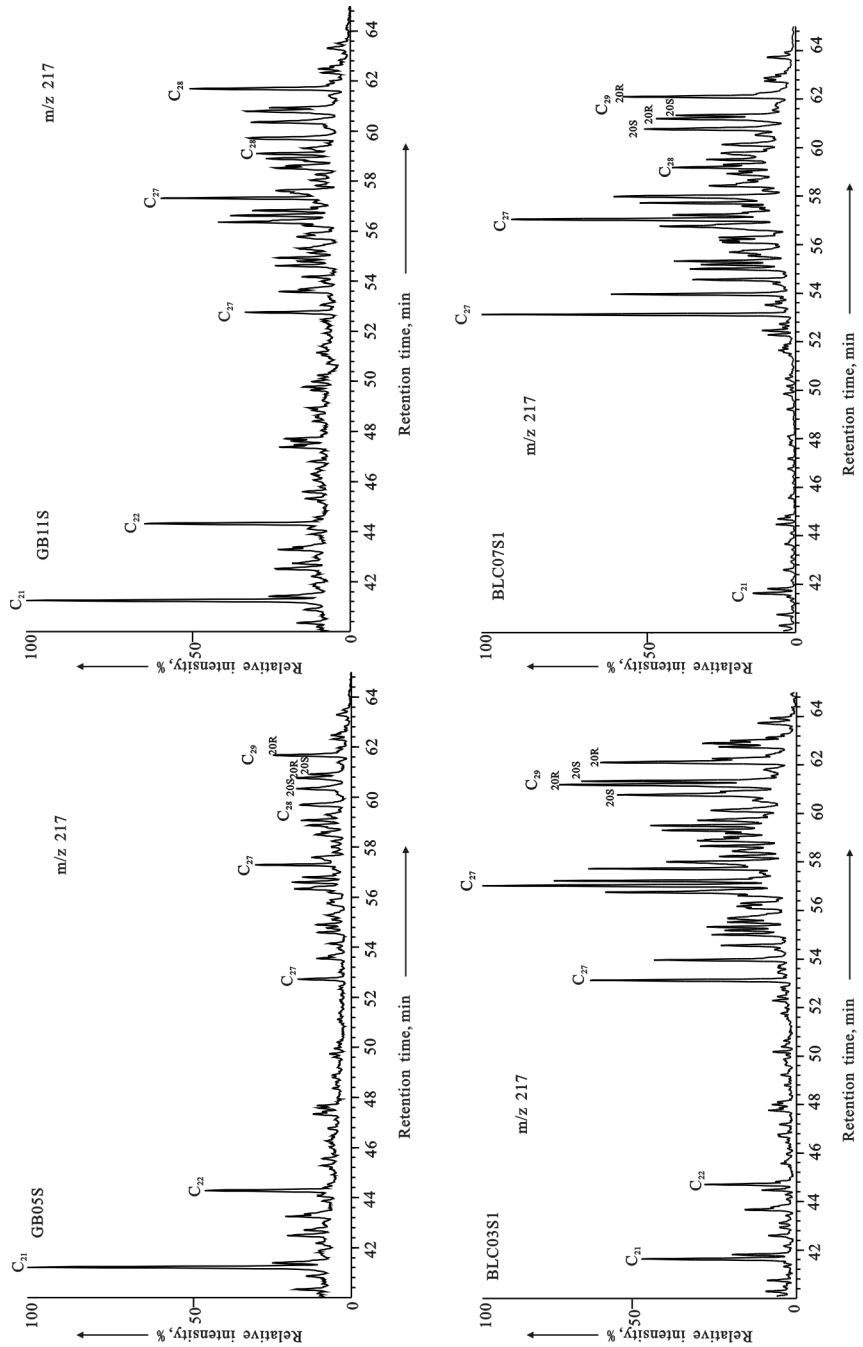

Fig. 5. m/z 217 chromatograms showing the relative abundance of steranes in the selected samples from the studied sections of the Qiangtang Basin. (Abbreviations used: GB – Ganbeixiama, BLC – Biluocou).

Table 4. Parameters of steranes of Lower Jurassic black shale in the Qiangtang Basin

Sample No	Lithology	Regular steranes ααα-20R, %			C_{27}/C_{29}	C_{21}regnanes/$C_{29}ααα$	$(C_{21}+C_{22})/C_{29}ααα$	C_{29}20S/(20S + 20R)	$C_{29}αββ/(αββ + ααα)$
		C_{27}	C_{28}	C_{29}					
GB05S	Shale	36	30	34	1.05	1.76	2.46	0.45	0.41
GB09S	Marl	38	28	34	1.11	1.40	2.03	0.44	0.39
GB10S	Shale	36	29	35	1.03	1.63	2.35	0.46	0.39
GB11S	Marl	34	31	35	0.99	0.90	1.38	0.43	0.40
BLC01S1	Oil Shale	27	32	41	0.65	0.20	0.25	0.57	0.65
BLC02S1	Shale	35	27	38	0.93	0.25	0.36	0.50	0.57
BLC02S2	Shale	41	24	35	1.20	0.44	0.63	0.53	0.57
BLC03S1	Mudstone	32	25	43	0.76	0.33	0.50	0.50	0.55
BLC03S2	Mudstone	30	27	44	0.68	0.28	0.43	0.48	0.53
BLC07S1	Mudstone	33	25	42	0.77	0.11	0.15	0.53	0.48
BLC08S1	Mudstone	32	29	39	0.82	0.13	0.18	0.59	0.53

Basin of northern Tibet is mainly algae with some contribution of land-based higher plants.

Based on thermodynamic activity, steranes generally undergo the following three changes in terms of organic matter maturity and evolution: configurational isomerization, aromatization and low-molecular-weight component accumulation [6, 33–35]. The ratios of C_{29} regular steranes ααα20S/(20S + 20R) and αββ/(αββ + ααα) are often used to assess maturity. In GB samples, the C_{29}ααα20S/(20S + 20R) steranes ratio varies from 0.43 to 0.46, and $C_{29}αββ/(αββ + ααα)$ from 0.39 to 0.41. At the same time, in BLC samples, C_{29}ααα20S/(20S + 20R) ranges from 0.50 to 0.59 (except for sample BLC03S2 whose respective value is 0.48), and $C_{29}αββ/(αββ + ααα)$ between 0.53 and 0.65 (except for sample BLC07S12 whose $C_{29}αββ/(αββ + ααα)$ is 0.48) (Table 4). These values demonstrate that the organic matter of BLC samples is in the stage of maturity, while its degree is higher than that of GB samples.

5. Conclusions

This paper discusses in detail the chacateristics of biomarkers of black shale from the Lower Jurassic Quse Formation in the Southern Qiangtang Depression of northern Tibet, including *n*-alkanes, acyclic isoprenoids, terpenoids and steranes. *n*-Alkanes are characterized by a typical unimodal distribution, with dominant low carbon numbers of nC_{16}–nC_{19}, which shows

that the organic matter sources are mainly algae and planktonic organisms along with terrestrial higher plants. Furthermore, such acyclic isoprenoid alkanes as pristane and phytane are detected as being the most abundant, while the phytane dominance suggests that organic matter deposited in a reducing environment. In addition, the maturity parameters show that the organic matter is in the maturity stage. So, it is concluded that the Lower Jurassic black shale resource system in the Qiangtang Basin of northern Tibet has a certain hydrocarbon potential.

Acknowledgements

The authors are grateful to Youjun Tang for performing the GC-MS analysis, and to Drs. Zhanhu Cai and Qilai Li for carrying out fieldwork. This research was financed by the National Natural Science Foundation of China (grants No. 41402099 and No. 41572095), the Open Foundation of the State Key Laboratory of Oil/Gas Reservoir Geology and Exploitation (Grant No. PLC 201603), and the Open Foundation of the Key Laboratory for Sedimentary Basins and Oil and Gas Resources of the Ministry of Land and Resources (Grant No. zdsys2014002).

REFERENCES

1. Wang, C. S., Yi, H. S., Li, Y. *Geology Evolution and Oil and Gas Prospect Evaluation of Qiangtang Basin in Tibet*. Geological Publishing House, Beijing, 2001 (in Chinese with English abstract).
2. Zhao, Z. Z., Li, Y. T., Ye, H. F. Zhang, Y. W. *Structural features and evolution of the Tibet plateau*. Science Press, Beijing, 2001, 23–25 (in Chinese with English abstract).
3. Chen, L., Yi, H. S., Hu, R. Z., Zhong, H., Zou, Y. R. Organic geochemistry of the Early Jurassic oil shale from the Shuanghu area in Northern Tibet and the Early Toarcian Oceanic Anoxic Event. *Acta Geol. Sin-Engl.,* 2005, **79**(3), 392–397.
4. Chen, L., Yi, H. S., Tsai, L. L. Y., Xu, G. W., Da, X. J., Lin, A. T. S. The Jurassic black shales facies from Qiangtang basin (northern Tibet): Rare earth and trace elements for palaeoceanographic implications. *Acta Geol. Sin-Engl.,* 2013, **87**(2), 540–554.
5. Chen, L., Jenkyns, H. C., Xu, G. W., Mattioli, E., Da, X. J., Yi, H. S., Xia, M. Q. Zhu, Z. X., Huang, Z. H. Preliminary nanofossil and geochemical data from Jurassic black shale from the Qiangtang basin, northern Tibet. *J. Asian Earth Sci.*, 2016, **115**, 257–267.
6. Yi, H. S., Chen, L., Jenkyns, H. C., Da, X. J., Xia, M. Q., Xu, G. W., Ji, C. J. The Early Jurassic oil shales in the Qiangtang basin, northern Tibet: biomarkers and Toarcian Oceanic Anoxic Events. *Oil Shale*, 2013, **30**(3), 441–455
7. Fu, X. G., Wang, J., Feng, X. L., Chen, W. B., Wang, D., Song, C. Y., Zeng, S. Q. Mineralogical composition of and trace-element accumulation in

lower Toarcian anoxic sediments: a case study from the Bilong Co. oil shale, eastern Tethys. *Geol. Mag.*, 2016, **153**(4), 618–634.
8. Ji, C. J., Xia, G. Q., Yi, H. S., Wu, X. H., Li, Q. L., Mao, L. L., Fang, C. G. Aromatic hydrocarbons in the Biluo Co oil shale of the Shuanghu area, Northern Tibetan Plateau, and their implications. *Oil Shale*, 2014, **31**(4), 351–364.
9. Wang, J., Tan, F. W., Li, Y. L., Li, Y. T., Chen, M., Wang, C. S., Guo, Z. J., Wang, X. L., Du, B. W., Zhu, Z. F. *The Potential of the Oil and Gas Resources in Major Sedimentary Basins on the Qinghai-Xizang (Tibet) Plateau*. Geological Publishing House, Beijing, 2004, 34–88 (in Chinese with English abstract).
10. Liu, Z. Q., Xu, X., Pan, G. T., Li, T. L., Yu, G. M., Yu, X. J., Jiang, X. Z., Wei, G. Y., Wang, C. S. *Tectonics, Geological Evolution and Genetic Mechanism of Qinghai-Xizang Plateau*. Geological Publishing House, Beijing, 1990 (in Chinese with English abstract).
11. Yu, G. M., Wang, C. S. *Sedimentary Geology of the Xizang (Tibet) Tethys*. Geological Publishing House, Beijing, 1990 (in Chinese with English abstract).
12. Matte, P., Tapponnier, P., Arnaud, N., Bourjot, L., Avouac, J. P., Vidal, P., Liu, Q., Pan, Y. S., Wang, Y. Tectonics of Western Tibet, between the Tarim and the Indus. *Earth. Planet. Sc. Lett.*, 1996, **142**(3–4), 311–330.
13. Li, C., He, Z. H., Yang, D. M. The Problems of Geological tectonics in the Qiangtang Area, Tibet. *Global Geology*, 1996, **15**(3), 18–23 (in Chinese with English abstract).
14. Jiang, M. Z., Wang, H. W. Aeromagnetic anomaly character in Qiangtang basin, northern Tibet. *Geological Science and Technology Information*, 2001, **20**(2), 95–99 (in Chinese with English abstract).
15. Yi, H. S., Lin, J. H., Zhao, B., Li, Y., Shi, H., Zhu, L. D. New biostratigraphic data of the Qiangtang area in the northern Tibetan plateau. *Geological Review*, 2003, **49**(1), 59–65 (in Chinese with English abstract).
16. Yin, J. R., Gao, J. H., Wang, Y. S., Zhang, S. Q., Zheng, C. Z., Xu, De. B., Bai, Z. D., Sun, X. Jurassic ammonites in anoxic black shales from Sewa and Anduo, Northern Tibet. *Acta Palaeontologica Sinica*, 2006, **45**(3), 311–331 (in Chinese with English abstract).
17. Yin, J. R., Sun, L. X., Bai, Z. D., Xu, D. B., Zhang, X. J. New data on the Jurassic ammonites from the Shuanghu and Amdo areas, with comments on the Jurassic strata in north Tibet. *Journal of Stratigraphy*, 2005, **29**(1), 7–15 (in Chinese with English abstract).
18. Wang, Y. S., Zheng, C. Z. Lithostratigraphy, sequence stratigraphy, and biostratigraphy of the Suobucha and Quse Formations and the Triassic-Jurassic boundary in the Sewa area on the south margin of the Qiangtang basin, northern Tibet. *Journal of Stratigraphy*, 2007, **31**(4), 377–384 (in Chinese with English abstract).
19. Wang, Y. S., Zheng, C. Z. Gypsum beds of the early Jurassic Quse Formation in the Biloucuo area of the southern Qiangtang basin, northern Xizang. *Journal of Stratigraphy*, 2008, **32**(3), 321–326 (in Chinese with English abstract).
20. Matsumoto, G. I., Akiyama, M., Watanuki, K., Torii, T. Unusual distributions of long-chain n-alkanes and n-alkenes in Antarctic soil. *Org. Geochem.*, 1990, **15**(4), 403–412.

21. Ficken, K. J., Li, B., Swain, D. L., Eglinton, G. An *n*-alkane proxy for the sedimentary input of submerged/floating freshwater aquatic macrophytes. *Org. Geochem.*, 2000, **31**(7–8), 745–749.
22. Nott, C. J., Xie, S., Avsejs, L. A., Maddy, D., Chambers, F. M., Evershed, R. P. *n*-Alkane distributions in ombrotrophic mires as indicators of vegetation change related to climatic variation. *Org. Geochem.*, 2000, **31**(2–3), 231–235.
23. Bingham, E. M., McClymont, E. L., Väliranta, H., Mauquoy, D., Roberts, Z., Chambers, F. M., Pancost, R. D., Evershed, R. P. Conservative composition of n-alkane biomarkers in Sphagnum species: implications for paleoclimate reconstruction in ombrotrophic peat bogs. *Org. Geochem.*, 2010, **41**(2), 214–220.
24. Rodriguez, N. D., Philp, R. P. Productivity and paleoclimatic controls on source rock character in the Aman Trough, north central Sumatra, Indonesia. *Org. Geochem.*, 2012, **45**, 18–28.
25. Maxwell, J. R., Cox, R. E., Ackman, R. G., Hooper, S. N. The diagenesis and maturation of phytol. The stereochemistry of 2,6,10,14-tetramethylpentadecane from an ancient sediment. In: *Advances in Organic Geochemistry* (von Gaertner, H. R., Wehner, H., eds.), Pergamon Press, Oxford, 1972, 277–291.
26. Powell, T. G., McKirdy, D. M. Relationship between ratio of pristane to phytane, crude oil composition and geological environment in Australia. *Nature*, 1973, **243**, 37–39.
27. Sinninghe Damsté, J. P., Kenig, F., Koopmans, M. P., Köster, J. G., Schouten, S., Hayes, J. M., De Leeuw, J. W. Evidence for gammacerane as an indicator of water column stratification. *Geochim. Cosmochim. Ac.*, 1995, **59**(9), 1895–1900.
28. Peters, K. E., Walters, C. C., Moldowan, J. M. *The Biomarker Guide: II. Biomarkers and Isotopes in Petroleum Exploration and Earth History*, 2nd ed. Cambridge University Press, Cambridge, 2005.
29. Rashby, S. E., Sessions, A. L., Summons, R. E., Newman, D. K. Biosynthesis of 2-methylbacteriohopanepolyols by an anoxygenic phototroph. *Proc. Nat. Acad. Sci.*, 2007, **104**(38), 15099–15104.
30. Aquino Neto, F. R., Trendel, J. M., Restle, A., Connan, J., Albrecht, P. A. Occurrence and formation of tricyclic and tetracyclic terpanes in sediments and petroleums. In: *Advances in Organic Geochemistry 1981* (Bjorøy, M. et al., eds.). Wiley and Sons, London, 1983, 659–667.
31. Huang, W. Y., Meinschein, W. G. Sterols as ecological indicators. *Geochim. Cosmochim. Ac.*, 1979, **43**(5), 739–745.
32. Volkman, J. K. Sterols and other triterpenoids: source specificity and evolution of biosynthetic pathways. *Org. Geochem.*, 2005, **36**(2), 139–159.
33. Seifert, W. K., Moldowan, J. M. Paleoreconstruction by biological markers. *Geochim. Cosmochim. Ac.*, 1981, **45**(6), 783–794.
34. Sachse, V. F., Littke, R., Jabour, H., Schümann, T., Kluth, O. Late Cretaceous (Late Turonian, Coniacian and Santonian) petroleum source rocks as part of an OAE, Tarfaya Basin, Morocco. *Mar. Petrol. Geol.*, 2012, **29**(1), 35–49.
35. Blumenberg, M., Thiel, V., Riegel, W., Kah, L. C., Reitner, J. Biomarkers of black shales formed by microbial mats, Late Mesoproterozoic (1.1 Ga) Taoudeni Basin, Mauritania. *Precambrian Res.*, 2012, **196–197**, 113–127.

Presented by A. Soesoo
Received April 16, 2016